

Study on the effects of monochromatic aberrations in the accommodation response by using adaptive optics

Enrique J. Fernández and Pablo Artal

Laboratorio de Optica, Departamento de Física, Universidad de Murcia, Campus de Espinardo (Edificio C), 30071 Murcia, Spain

Received January 3, 2005; revised manuscript received February 28, 2005; accepted March 4, 2005

The effect of asymmetric monochromatic aberrations in the accommodation response was studied by using an adaptive optics (AO) system. This approach permits the precise modification of ocular aberrations during accommodation. The AO system is composed of a real-time Hartmann–Shack wavefront sensor and a membrane deformable mirror with 37 independent actuators. The accommodation response was measured in two subjects with their normal aberrations and with the asymmetric aberrations terms corrected. We found a significant and systematic increase in the response accommodation time, and a reduction in the peak velocity, in both subjects when the aberrations were corrected in real time. However, neither the latency time nor the precision of the accommodation were affected. These results may indicate that the monochromatic aberrations play a role in driving the accommodation response. © 2005 Optical Society of America

OCIS codes: 010.1080, 330.5370, 330.7310.

1. INTRODUCTION

Adaptive Optics (AO) permits the measurement and correction of wavefront aberrations in real time. Originally developed to compensate the images for atmospheric turbulence in both the military and the astronomical fields,¹ the reduction in the cost of the technology has extended its use to other research areas. AO is the best solution in those situations where image quality is degraded dynamically. This is the case in the optics of the human eye, where the aberrations change continuously over time.² Attempts to surmount the limitations imposed by the ocular aberrations in retinal imaging by using speckle interferometric techniques³ were first suggested in the late 1980s. In the same year, also reported was the use of a deformable mirror for the static compensation of the low-order ocular aberrations in a scanning laser ophthalmoscope.⁴ During the next decade, static high-order aberrations correction in the human eye was demonstrated,⁵ and real-time closed-loop aberration corrections (AO, strictly speaking) in the living eye using deformable mirrors were also recently reported.^{6,7} Although deformable mirrors remain the most widely used correctors, the use of other devices, such as liquid crystal spatial modulators, has also been explored to compensate the eye's aberrations.^{8,9}

AO techniques can contribute to the study of different aspects of human vision. The correction of ocular aberrations notably increases the quality of the retinal images obtained with ophthalmoscopes. This approach may allow detection of some retinal features in the living eye that are undetectable with traditional imaging methods. AO has already been incorporated successfully in flood-illumination fundus cameras,¹⁰ scanning laser ophthalmoscopes,^{11,12} and more recently in ultra-high-resolution optical coherence tomography.¹³ Nevertheless,

retinal imaging is not the only application of AO in vision science. By permitting the subject to perform visual tests through the AO system, the experimenter can both control and modify all the optical parameters objectively. This ability to measure and correct for ocular aberrations simultaneously with the accomplishment of visual tests can be regarded as an "AO visual simulator"^{14,15} and be applied in a large variety of experiments. As an example, this type of approach was recently used to discover a neural adaptation in the visual system to the particular eye's aberrations.^{14,16}

In this paper, we propose the use of AO techniques to study how high-order asymmetric aberrations affect the accommodation response. Despite the fact that the mechanism of accommodation in the human eye has been studied widely for decades, there are still questions that remain unsolved and even in some cases are subjects of controversy. Accommodation permits us to keep in good focus the images of stimuli placed at different distances from the eye. Defocus alone does not provide information about the direction of accommodation.^{17,18} However, under normal conditions the eye correctly accommodates to the right focus. In consequence, a number of cues help to indicate to the system the appropriate direction for minimizing defocus in the retinal images. It has been demonstrated extensively that subjective distance perception, knowledge of the target size, and perspective and convergence are cues used for accommodation.¹⁹ Cues of an optical nature also play an important role in the process: ocular chromatic aberration,^{20,21} microfluctuations of accommodation,^{22,23} and eye movements during fixation. Concerning the role that monochromatic aberrations play in accommodation, it was early recognized that spherical aberration introduces asymmetries in the retinal images that may serve to indicate the correct direction of the

accommodation.²⁴ The possible role of other monochromatic aberrations serving as a cue to the accommodation is not completely understood yet. Wilson *et al.*²⁵ recently studied the sensitivity of the eye in subjectively discriminating the asymmetries in the retinal images caused by higher-order monochromatic aberrations. They demonstrated the ability in several subjects to detect asymmetries in the ocular point-spread function (PSF) as well as in more complex targets such as letters. A better discrimination in the direction of the defocus was achieved by incrementing the amount of monochromatic aberrations. These results indicate that monochromatic aberrations may play an active role in the accommodation mechanism.

In this context, the aim of this study is to further elucidate how monochromatic aberrations affect the accommodation response. We used an AO system specially dedicated to measuring some properties of the accommodation response for different optical conditions, in particular when subjects accommodated either with their natural aberrations or with their asymmetric aberrations partially removed.

2. METHODS

A. Experimental AO System

The AO system used here includes as main components a Hartmann–Shack (HS) wavefront sensor²⁶ and a membrane deformable mirror.²⁷ Figure 1 shows a schematic diagram of the experimental apparatus. The HS sensor uses a CCD camera operating at 25 Hz and an array of square microlenses (of 0.4 and 6.4 mm focal length) placed in front of the camera. The HS images are analyzed fast enough by the control PC to estimate the eye's aberrations from each frame in real time (25 Hz). A He–Ne laser ($\lambda=633$ nm) is used for system alignment and calibration. The membrane deformable mirror has 37 independent electrodes beneath the mirrored surface that can be independently driven by the computer while the membrane remains grounded. The electrostatic force induced between the mirror and the electrodes deforms the flexible membrane toward its base. The control of this device and its performance for experiments in the human eye has been described elsewhere.²⁷ Voltages applied to 37 control electrodes electrostatically drive the membrane shape. Since the force between the membrane and the electrodes is attractive, the membrane can be pulled only toward its base. By biasing the mirror to a nonzero voltage, deformation in both directions can be induced. To control the mirror, the influence functions were determined by applying voltages to each electrode sequentially while measuring the produced wavefront with the HS sensor. The surface's wavefronts are expressed as Zernike's polynomial expansion using 21 terms, which corresponds to the fifth order. The influence functions are grouped in the influence function matrix (IFM) by columns. The dimension of the matrix IFM is 21×37 : the number of Zernike modes and the number of electrodes. Assuming linear response, the control matrix is obtained simply as the inverse of the IFM. In general, this matrix is not regular, so pseudoinversion methods are required.

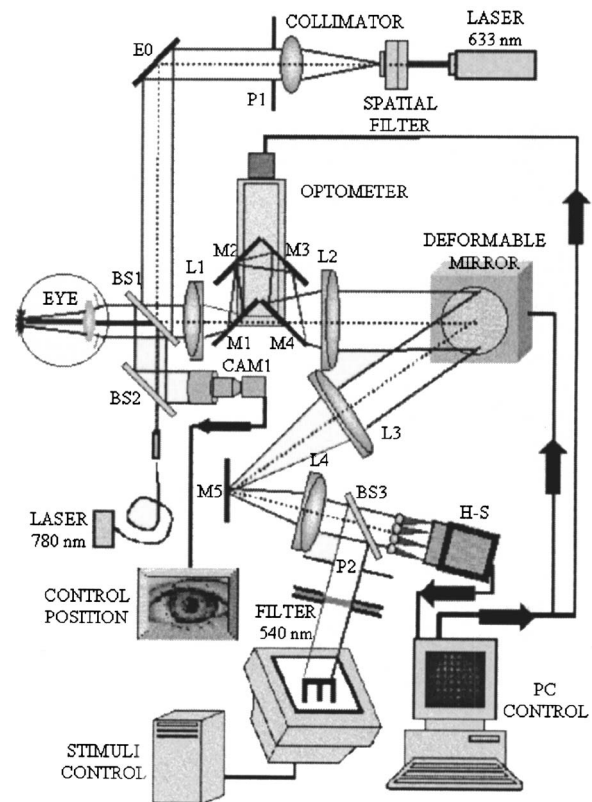


Fig. 1. Experimental apparatus. A pigtailed near infrared laser is used as the beacon source for the eye. A Hartmann–Shack (H-S) wavefront sensor measures the ocular aberrations in real time (25 Hz). The deformable mirror modifies the ocular aberrations in closed-loop. During the measurements the apparatus allows the subject to view visual stimuli simultaneously. The motorized optometer can generate abrupt changes in defocus, inducing accommodation in the subject.

The subject is fixated by using a bite bar mounted in a 3-D micropositioner. The pupil centering is performed by means of an auxiliary camera, CAM1, focused at the focal plane of lens L1. The exit pupil of the eye is conjugated with both the deformable mirror and the microlens array by means of lenses L1, L2 ($f'_1=120$ mm; $f'_2=200$ mm) and lenses L3, L4 ($f'_3=200$ mm; $f'_4=100$ mm). These lenses were selected to produce appropriate magnification among the three conjugate planes: an eye pupil diameter of 5.52 mm permits filling of the optimum controllable area on the deformable mirror (9.2 mm diameter) and the CCD camera area used by the HS sensor (4.8 mm diameter). A pigtailed near-infrared diode laser illuminates the subject's eye with a diameter of 1.75 mm. To remove the corneal reflection from the HS images, the illumination beam is slightly misaligned. During the measurements, light intensity is limited to $5 \mu\text{W}/\text{cm}^2$, ~ 3 orders of magnitude below the maximum exposure limit for continuous viewing.²⁸ This permits long time exposures, which are important in our experiment, where subjects are asked to accommodate while the aberrations are continuously measured and modified. The system incorporates a motorized optometer to correct or add defocus independently of the deformable mirror. The optometer consists of four mirrors, two of them—M2 and M3—mounted on a mobile and motorized platform controlled remotely by the com-

puter. The precision of the movements is $2.5\text{ }\mu\text{m}$, which corresponds to 5×10^{-4} diopters (D) of defocus. The speed and acceleration of the motorized translation stage was adjusted to provide changes in object vergence that were much faster than typical eye's response. An additional beam splitter, BS3, permits the subject to see visual stimulus while the aberrations are being modified. A 4.8-mm-diameter aperture, P2, placed at the focal distance of lens L4 matches the same aperture as that selected in the HS image to compute the aberrations. An interference filter centered at 540 nm with 10 nm bandwidth is used to present quasi-monochromatic stimuli: a high-contrast letter E displayed on a high-fidelity monitor subtending approximately 30 arcmin with an effective luminance of 35 cd/m^2 .

B. Experimental Protocol

Two subjects with normal vision (PA and SM, aged 40 and 29 years old, 1.5 and 3 D of refractive errors respectively) participated in this study. Both subjects were familiar with the purpose of the experiment and the methods. After the eye is centered with respect to the instrument axis, the subject is asked to look for the best subjective focus by adjusting the motorized optometer. Once the best subjective focus is found, the eye's aberrations are measured in real time while the subject is looking at the stimulus. We tested the possible influence of the asymmetric aberrations on the accommodation responses by inducing abrupt changes in the vergence of the stimulus and recording the aberrations, including defocus, when the subject tried to follow the stimulus. This procedure was repeated both with the normal aberrations in the eye and with all the asymmetric aberrations removed by the deformable mirror. These changes in vergence were 1.5 and 2 D for subjects PA and SM, respectively. The procedure was as follows: While the subject was looking at the stimulus through the AO system, at a given time unexpected by the subject the optometer abruptly changed the vergence of the stimulus from far (unaccommodated eye) to near (1.5 or 2 D). The measurements were repeated under two different situations: the normal and the corrected case. In the former, the deformable mirror is set to correct only the aberrations introduced by the system statically. Consequently, the subject will perform the accommodation experiments solely with his normal aberrations (referred in the following as normal case). In the other situation, in addition to correcting the system's aberrations the deformable mirror also continuously compensates (in real time and closed loop) the asymmetric aberrations of the eye while the subject accommodates. The subject will perform the accommodation experiments with only his symmetric aberrations left uncorrected (referred in the following as corrected case). Specifically, we corrected astigmatism (Z_3 and Z_5) and third-order asymmetric terms: coma (Z_7 and Z_8) and trefoil (Z_6 and Z_9). The subjects were completely unaware of which of these two cases, normal or corrected, was being performed during their accommodation experiments. For subject PA there were six runs, half of them with the aberrations corrected and the rest under natural viewing conditions. The accommodative responses of subject SM were measured

during the experiment eight times, where four corresponded to the natural case and the others with the aberrations corrected.

3. RESULTS

Figure 2 shows an example of the root mean squared (RMS) of the aberrations (except defocus) for each subject, with and without correction of the asymmetric aberrations, while the subjects were performing one of the accommodation experiments. The origin in the temporal axis corresponds to the beginning of the change in the vergence of the stimulus. The triangles represent the case with dynamic correction of the asymmetric terms, and the squares are for the normal case. In subject SM, RMS in the normal case increases slightly with accommodation, while in subject PA it remains stable. The AO system permits reasonably stable aberrations (RMS) to be maintained for the corrected case in both subjects while they are accommodating. Figure 3 shows the modulus- 2π representation of the wave aberrations (without defocus) for subject PA for the normal and corrected cases, with the associated PSFs. As an estimation of the retinal images quality, the corresponding Strehl ratios have been added on every PSF plot. There are two maps for every case (normal and corrected) showing the aberrations for both unaccommodated and accommodated cases. The same type of results for subject SM is presented in Fig. 4. These figures show nicely the correction of the asymmetric aberrations during the accommodation experiments. For both subjects, the retinal image remains rotationally symmetric in that case during the accommodation. For the normal case, the retina image is clearly asymmetric and the aberrations change during accommodation in a different manner for each subject, as previously reported.^{29,30} To better quantify the aberration changes occurring during accommodation, Figs. 5 and 6 show the values of the

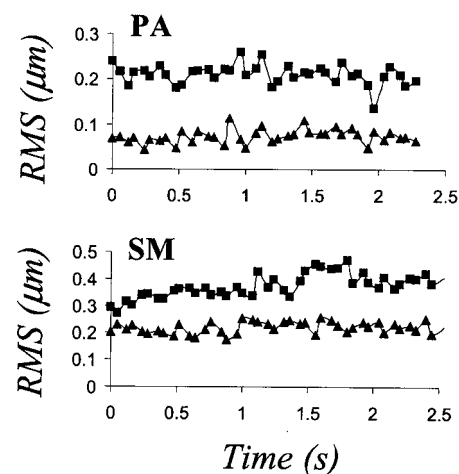


Fig. 2. Evolution of the average RMS of the ocular aberrations for subjects PA and SM during accommodation in a 5.52 mm pupil. Experimental data are shifted in the temporal axis to perform the average, so that the origin in this axis matches the exact starting point for the induced changes in the defocus. Triangles, RMS when the accommodation is performed under natural viewing conditions (natural aberrations); squares, closed-loop asymmetric-aberration correction.

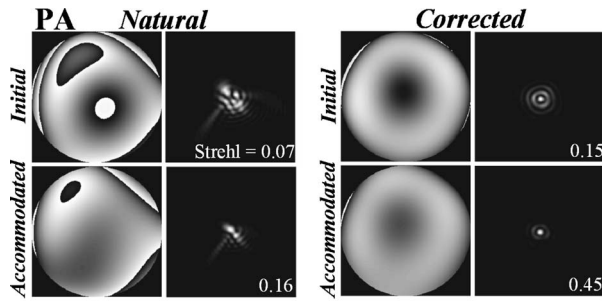


Fig. 3. Average ocular aberrations (modulus- 2π representation) for subject PA before and during the induced 1.5 D accommodation in a 5.52 mm pupil. (a) The natural case shows the measured aberrations when the subject performs the accommodation under natural viewing conditions. (b) The corrected case presents the aberrations when the asymmetric aberrations are corrected. In both cases the associated PSFs are shown together with the estimated Strehl ratios. The tilt terms and defocus are not included in the aberrations maps.

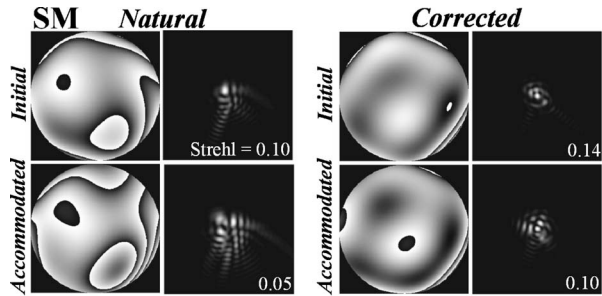


Fig. 4. Average ocular aberrations (modulus- 2π representation) for subject SM before and during the induced 2.0 D accommodation in a 5.52 mm pupil. (a) and (b) as in Fig. 3.

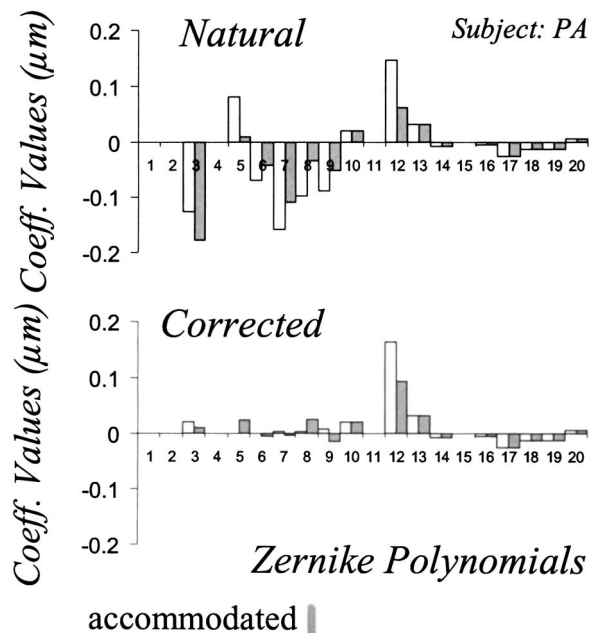


Fig. 5. Average ocular aberrations, excluding defocus and tilt, in subject PA before (white bars) and during (shaded bars) the 1.5 D induced accommodation for both the natural and the corrected cases. The aberrations are expressed in terms of the Zernike polynomial expansion following the OSA standard ordering.

Zernike terms for each subject in the two accommodation states and in the natural and corrected cases. These plots show that the asymmetric terms are well corrected within the capability of the corrected device.²⁷ Spherical aberration changed in a similar way in both subjects and in the two conditions, becoming less positive with accommodation. It must be noted (and will be discussed in more detail below) that spherical aberration was not corrected mainly because of the limitations of the device used.

The accommodation response was measured for each experimental condition. From these responses (defocus as a function of time after the abrupt change of the stimulus vergence), a series of selected parameters were obtained: latency time, defined as the time delay measured between the change of vergence of the stimulus and the beginning of the accommodation; accommodation response time, defined as the time that the eye is continuously varying the focus, from the initial state to the finally accommodated state reached; and accommodation error, defined as the difference between the ideal response, corresponding to the case of perfect focusing, and the reached steady state. The peak velocity in the response was also obtained. To extract all these parameters, the experimental data of the accommodation response were fitted to a Boltzmann sigmoidal function, given by

$$y = \frac{A_1 - A_2}{1 + \exp[(x - x_0)/dx]} + A_2, \quad (1)$$

with A_1 , A_2 , d_x and x_0 the fitting parameters. The values for A_1 and A_2 correspond to the initial (before accommodation) and the final defocus (after accommodation), respectively. Figure 7 shows the measured accommodation response as a function of time in subject PA for a 1.5 D abrupt change of vergence (circles). The temporal axis has been shifted so that the value zero corresponds to the

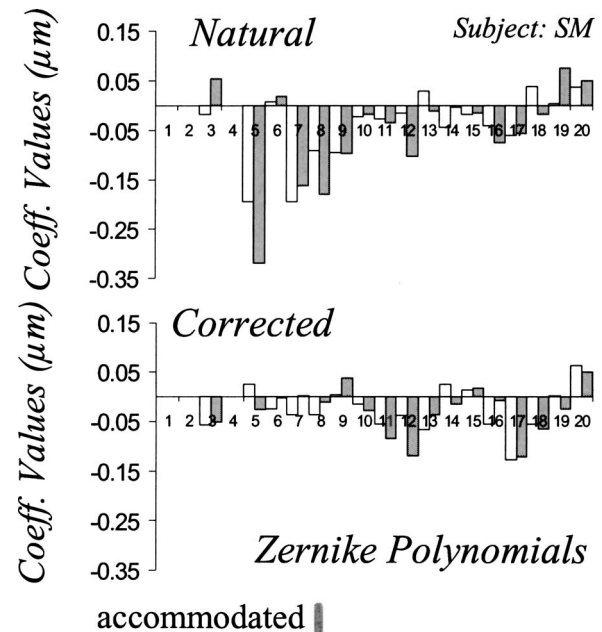


Fig. 6. Average ocular aberrations, excluding defocus and tilt, in subject SM before (white bars) (shaded bars) and during the 2 D induced accommodation for both the natural and the corrected cases.

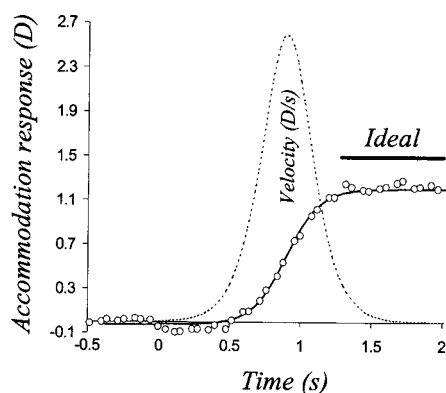


Fig. 7. Accommodation response as a function of time for subject PA induced by a 1.5 D abrupt change in defocus (circles). The data are shifted so that the value 0 in time matches the origin of the change of defocus. The thick solid line represents the ideal final accommodation (1.5 D). The thin solid curve shows the sigmoidal fit obtained from the experimental data. The dashed curve shows the velocity of the accommodation (in diopters per second), calculated as the first derivative of the estimated sigmoidal function.

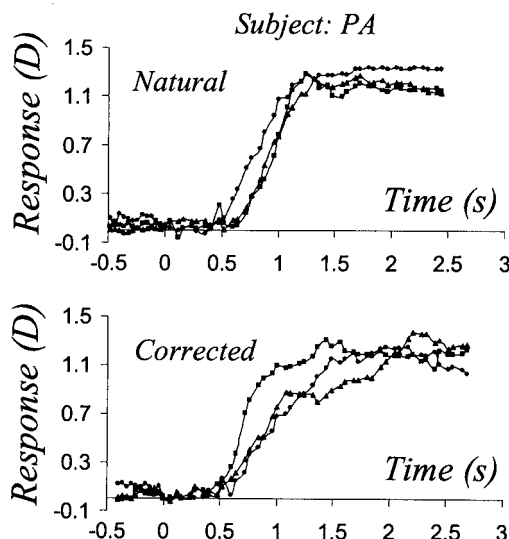


Fig. 8. Accommodation responses in subject PA under natural viewing conditions (top) and with asymmetric aberration correction (bottom). The programmed step change in defocus was 1.5 D. The experimental data are shifted on the temporal axis so that the zero value corresponds to the beginning of the defocus change.

abrupt change of vergence of the stimulus. The sigmoidal fit is represented by the solid curve. The velocity of the accommodation response, in diopters per second, is obtained as the first derivative of the sigmoidal function fitted to the data (dashed curve in Fig. 7). The peak velocity is determined as the maximum of the accommodation velocity. The full accommodation change is the difference between the initial and the final defocus in the eye. We considered that the accommodation ramp starts when the defocus reaches 2% of the total accommodation change and finishes at 98%. Following this criterion, the latency is the temporal interval between the change of vergence of the stimulus and the beginning of the accommodation ramp. We evaluated the quality of the fit of the sigmoidal func-

tion to the experimental data of the accommodation response by calculating the chi square parameter (χ^2). For subjects PA and SM, χ^2 ranged from 0.0016 to 0.0079 and from 0.007 and 0.048, respectively (for a perfect fit χ^2 is zero). These values support the choice of a sigmoidal function to fit the experimental data of the accommodation response over exponential functions.

Figure 8 shows all the measured accommodation responses for subject PA for both the case with his normal aberrations and the case with the symmetric aberration terms corrected in closed loop. The correction of the asymmetric aberrations appears to produce a less abrupt (slower) accommodative response. This tendency is also apparent in subject SM (Fig. 9). The accommodation stimuli were 1.5 and 2 D for subjects PA and SM, respectively. For every response the corresponding sigmoidal fit was performed and the parameters obtained. Figures 10 and 11 show the results for both subjects and the two conditions. The bar diagram on the left side of Fig. 10 presents the final level of accommodation in each subject with (gray) and without (white) asymmetric aberration correction. The dotted lines indicate the ideal response. In the two subjects, the achieved level of accommodation was not affected by the correction of the asymmetric terms. This indicates that the precision in the accommodation response seems to be unaffected by the correction of the asymmetric monochromatic aberrations. The panel on the right side of Fig. 10 presents the latency time for both subjects. Although the latency time is significantly different between subjects, the corrected and the natural cases show similar values. Figure 11 presents the accommodation response time and the response velocity. The response time increases for both subjects when the asymmetric aberrations were corrected. This increase is significant in both subjects (a factor of 4 and 2 for subjects SM and PM, respectively). This increase in the temporal response together with the fact that the final level of accommodation did not change explains the measured change in the velocity of the accommodative response.

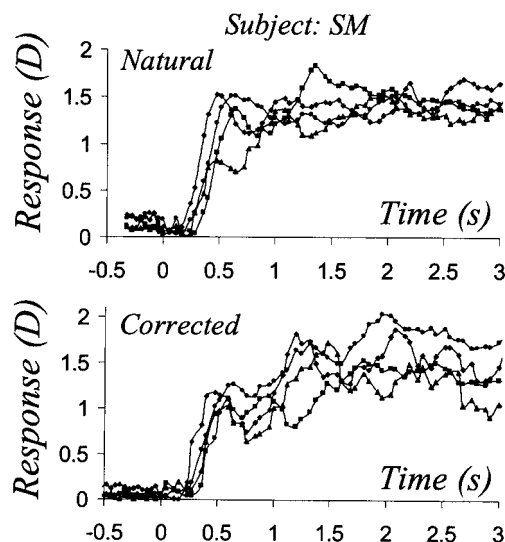


Fig. 9. Accommodation responses in subject SM under natural viewing conditions (top) and in the corrected case (bottom). The induced change in defocus was 2.0 D.

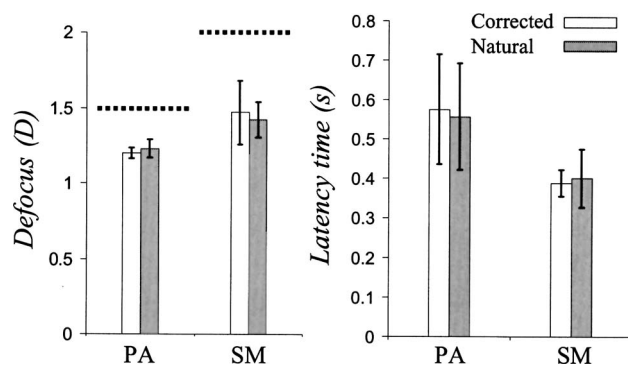


Fig. 10. Average results from the accommodation responses in the two subjects. In the left panel, the bars show the finally achieved accommodation with natural aberrations (gray) and with asymmetric-aberration correction (white). The right panel shows the latency time in the two cases. The error bars represent the standard deviation.

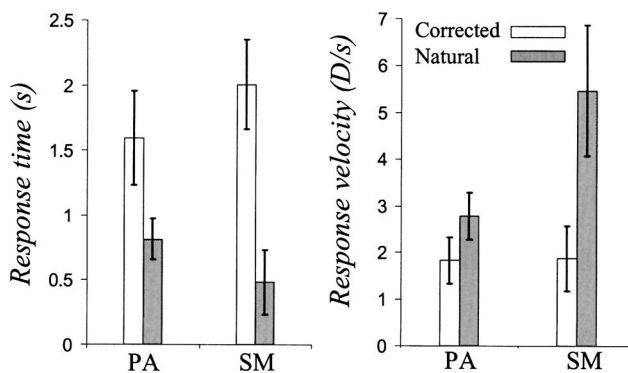


Fig. 11. Response time with natural aberrations (left panel, gray) and with asymmetric-aberration correction (white). The right panel shows the accommodation velocity in the two cases.

The panel on the right side of Fig. 11 shows the response velocity (in diopters/seconds) for both subjects and conditions. The relative decreases of the speed of the response when the asymmetric aberrations were corrected were 3 and 1.5 for SM and PA, respectively.

4. DISCUSSION

We found that the spherical aberration changes in the two subjects during the accommodation, becoming less positive. This has been a well-known fact ever since the first studies measuring aberrations in the eye.^{31,32} Although spherical aberration and its possible changes during accommodation may play a role in accommodation, in this study we concentrated only on the effect of asymmetric aberration terms. The rationale for this decision was twofold. On the one hand, we had a technical limitation in the degree of spherical aberration correction imposed by the membrane mirror; on the other hand, we decided to explore the effect of only asymmetric terms, minimizing the variations in the symmetry of the retinal images during accommodation. We achieved a quite good correction of asymmetric aberrations when the accommodation experiments were performed. As far as we know, this was the first attempt to use closed-loop AO to perform accommodation experiments. Because of the technical difficulties

of this experiment, we limited our study to two subjects. Although this would limit the conclusion to a general population, we were more interested in showing the potential of the approach.

In the two subjects, both the accommodation response and the latency time were unaffected by the correction of asymmetric aberration. Nonetheless, we found a significant increment in the response time when the subjects performed the experiment with their asymmetric aberrations corrected. As there are related parameters, the speed of the response also decreased with the aberrations corrected. These changes in the response time and the peak velocity when the aberrations were removed may indicate the existence of a complex relationship between monochromatic aberrations and accommodation. This further supports the existence of a feedback-loop mechanism based on the asymmetric aberration terms that drives the accommodation response. A recent study²⁵ showed that the subjects were able to identify the correct direction of defocus solely using the information on monochromatic aberrations. If these aberrations helped the visual system to choose the appropriate direction of accommodation, it would not be surprising that when they were removed, the performance of the accommodation also would decrease. Although in our experiments the subjects always knew the direction of the accommodation (from far to near), the possible feedback loop may become impaired by the elimination of the asymmetric aberrations terms. In this case, perhaps the addition of a particular aberration that introduces more asymmetry in the retinal images while keeping the optical quality acceptable for the subject could improve the accommodation time.

This proposed scenario becomes highly complicated when other factors are considered. Recently a novel effect in vision related to monochromatic aberrations has been reported.^{14,16} It was found that the subjects exhibit a significant neural adaptation to their monochromatic aberrations. When the ocular aberration pattern is changed, even if the optical quality of the retinal image is preserved, the subjects suffer a notable decrease in vision. Moreover, this effect is expected also to occur when the optical quality of the retinal images is not maintained at all, as is the case in our experiment. The possible enhancement of the retinal image quality produced by the partial correction of the aberrations could be balanced by the change of the perceived ocular aberrations. This neural effect may partially contribute to the obtained results.

In summary, we demonstrated the potential of using an AO apparatus to explore the role of monochromatic aberrations during accommodation. When we partially removed asymmetric aberrations, we found a systematic reduction in the performance of accommodation. To our knowledge, these findings are the first experimental evidence that the correction of some high-order monochromatic aberrations may produce a deterioration of a particular visual function, accommodation. These results suggest that a hypothetical perfect real-time correction of normal aberrations could induce a collateral reduction in accommodation performance. However, it should be noted that accommodation involves, and is affected by, a large variety of factors, showing important intersubject variability. Therefore, future studies should incorporate a

larger number of subjects and different accommodation stimuli. As an example, Chen and colleagues³³ found no significant changes in the accommodation response when correcting all the monochromatic aberrations in a smaller range of defocus (± 0.5 D) and using a different accommodation stimulus. Further investigations using AO are needed to increase our understanding of the actual role of high-order monochromatic aberrations in the accommodation mechanism.

ACKNOWLEDGMENTS

This research was supported by Ministerio de Educacion y Ciencia, Spain (grants BFM2001-0391 and FIS2004-02153). A preliminary report³⁴ of this study was presented at the ARVO meeting, 2002, Fort Lauderdale, Florida, USA. The authors thank P. Kruger and D. Williams for helpful discussions about this work and S. Manzanera for serving as a subject.

The authors can be reached by e-mail: enriquej@um.es and pablo@um.es.

REFERENCES

1. H. W. Babcock, "The possibility of compensating astronomical seeing," *Publ. Astron. Soc. Pac.* **65**, 229–236 (1953).
2. H. Hofer, P. Artal, B. Singer, J. L. Aragon, and D. R. Williams, "Dynamics of the eye's wave aberration," *J. Opt. Soc. Am. A* **18**, 1–10 (2001).
3. P. Artal and R. Navarro, "High-resolution imaging of the living human fovea: measurement of the intercenter cone distance by speckle interferometry," *Opt. Lett.* **14**, 1098–1100 (1989).
4. A. W. Dreher, J. F. Bille, and R. N. Weinreb, "Active optical depth resolution improvement of the laser tomographic scanner," *Appl. Opt.* **28**, 804–808 (1989).
5. J. Liang, D. R. Williams, and D. Miller, "Supernormal vision and high resolution retinal imaging through adaptive optics," *J. Opt. Soc. Am. A* **14**, 2884–2892 (1997).
6. E. J. Fernández, I. Iglesias, and P. Artal, "Closed-loop adaptive optics in the human eye," *Opt. Lett.* **26**, 746–748 (2001).
7. H. Hofer, L. Chen, G. Y. Yoon, B. Singer, Y. Yamauchi, and D. R. Williams, "Improvement in retinal image quality with dynamic correction of the eye's aberrations," *Opt. Express* **8**, 631–643 (2001).
8. F. Vargas-Martín, P. Prieto, and P. Artal, "Correction of the aberrations in the human eye with liquid crystal spatial light modulators: limits to the performance," *J. Opt. Soc. Am. A* **15**, 2552–2562 (1998).
9. P. Prieto, E. J. Fernández, S. Manzanera, and P. Artal, "Adaptive optics with a programmable phase modulator: applications in the human eye," *Opt. Express* **12**, 4059–4071 (2004).
10. A. Roorda and D. R. Williams, "The arrangement of the three cone classes in the living human eye," *Nature (London)* **397**, 520–522 (1999).
11. A. Roorda, F. Romero-Borja, W. J. Donnelly III, H. Queener, T. J. Hebert, and M. C. W. Campbell, "Adaptive optics scanning laser ophthalmoscopy," *Opt. Express* **10**, 405–418 (2002).
12. B. Vohnsen, I. Iglesias, and P. Artal, "Confocal scanning laser ophthalmoscope with adaptive optics wavefront correction," in *Three-Dimensional and Multidimensional Microscopy: Image Acquisition and Processing X*, J.-A. Conchello, C. J. Cogswell, and T. Wilson eds., *Proc. SPIE* **4964**, 24–32 (2003).
13. B. Hermann, E. J. Fernández, A. Unterhuber, H. Sattmann, A. F. Fercher, W. Drexler, P. M. Prieto, and P. Artal, "Adaptive-optics ultrahigh-resolution optical coherence tomography," *Opt. Lett.* **29**, 2142–2144 (2004).
14. E. J. Fernández, S. Manzanera, P. Piers, and P. Artal, "Adaptive optics visual simulator," *J. Refract. Surg.* **18**, 634–638 (2002).
15. P. Piers, E. J. Fernández, S. Manzanera, S. Norrby, and P. Artal, "Adaptive optics simulation for intraocular lenses with modified spherical aberration," *Invest. Ophthalmol. Visual Sci.* **45**, 4601–4610 (2004).
16. P. Artal, L. Chen, E. J. Fernández, B. Singer, S. Manzanera, and D. R. Williams, "Neural compensation for the eye's optical aberrations," *J. Vision* **4**, 281–287 (2004).
17. L. Stark and Y. Takahashi, "Absence of an odd-error signal mechanism in human accommodation," *IEEE Trans. Biomed. Eng.* **12**, 138–146 (1965).
18. L. M. Smithline, "Accommodative response to blur," *J. Opt. Soc. Am.* **64**, 1512–1516 (1974).
19. K. F. Ciuffreda, "Accommodation and its anomalies," in *Vision and Visual Dysfunction*, J. R. Cronly-Dillon, ed. (Macmillan, 1991).
20. P. B. Kruger, S. Mathews, K. R. Aggarwala, and N. Sánchez, "Chromatic aberration and ocular focus: Fincham revisited," *Vision Res.* **33**, 1397–1411 (1993).
21. K. R. Aggarwala, E. S. Kruger, S. Mathews, and P. B. Kruger, "Spectral bandwidth and ocular accommodation," *J. Opt. Soc. Am. A* **12**, 450–455 (1995).
22. F. W. Campbell and G. Westheimer, "Factors influencing accommodation responses of the human eye," *J. Opt. Soc. Am.* **49**, 568–571 (1959).
23. W. N. Charman and G. Heron, "Fluctuations in accommodation: a review," *Ophthalmic Physiol. Opt.* **8**, 153–164 (1988).
24. E. F. Fincham, "The accommodation reflex and its stimulus," *Br. J. Ophthalmol.* **35**, 5–80 (1951).
25. B. J. Wilson, K. E. Decker, and A. Roorda, "Monochromatic aberrations provide an odd-error cue to focus direction," *J. Opt. Soc. Am. A* **19**, 833–839 (2002).
26. P. M. Prieto, F. Vargas-Martín, S. Goelz, and P. Artal, "Analysis of the performance of the Hartmann-Shack sensor in the human eye," *J. Opt. Soc. Am. A* **17**, 1388–1400 (2000).
27. E. J. Fernández and P. Artal, "Membrane deformable mirror for adaptive optics: performance limits in visual optics," *Opt. Express* **11**, 1056–1069 (2003).
28. American National Standard Institutes "For the safe use of lasers," ANSI Z136.1-2000, Laser Institute of America, (Orlando, Fla., 2000).
29. P. Artal, E. J. Fernández, and S. Manzanera, "Are optical aberrations during accommodation a significant problem for refractive surgery?" *J. Refract. Surg.* **18**, 563–566 (2002).
30. H. Cheng, J. K. Barnett, A. S. Vilupuru, J. D. Marsack, S. Kasthurirangan, R. A. Applegate, and A. Roorda, "A population study on changes in wave aberrations with accommodation," *J. Vision* **4**, 272–280 (2004).
31. A. Ivanoff, "About the spherical aberration of the eye," *J. Opt. Soc. Am.* **46**, 901–903 (1956).
32. T. C. Jenkins, "Aberrations of the eye and their effects on vision: 1. Spherical aberration," *Br. J. Physiol. Opt.* **20**, 59–91 (1963).
33. L. Chen, P. B. Kruger, and D. R. Williams, "Accommodation without higher order monochromatic aberrations," *Invest. Ophthalmol. Visual Sci. Suppl.* **43**, 956 (2002).
34. E. J. Fernández and P. Artal, "Adaptive-optics correction of asymmetric aberrations degrades accommodation," *Invest. Ophthalmol. Visual Sci. Suppl.* **43**, 954 (2002).